


A simple novel approach for detecting blood–brain barrier permeability using GPCR internalization

Z. Csaba^{*,1}, T. Vitalis^{*,1}, C. Charriaut-Marlangue^{*}, I. Margaill[†], B. Coqueran[†], P.-L. Leger^{*}, I. Parente^{*}, A. Jacquens^{*}, L. Titomanlio^{*}, C. Constans[‡], C. Demene[‡], M. D. Santin[§], S. Lehericy[§], N. Perrière[¶], F. Glacial[¶], S. Auvin^{*}, M. Tanter[‡], J.-F. Gherzi-Egea^{**}, H. Adle-Biassette^{*††}, J.-F. Aubry[‡], P. Gressens^{*} and P. Dournaud^{*} 

^{*}NeuroDiderot, Inserm U1141, Université de Paris, Paris, France, [†]Research Team "Pharmacology of Cerebral Circulation" EA4475, Faculté de Pharmacie de Paris, Université de Paris, Paris, France, [‡]Institut Langevin, ESPCI Paris, PSL Research University, CNRS UMR7587, Inserm U979, Inserm Technology Research Accelerator in Biomedical Ultrasound, Université de Paris, Paris, France, [§]Brain and Spine Institute-ICM, Center for NeuroImaging Research – CENIR, Sorbonne Paris Cité, UPMC Université Paris 06, Inserm U1127, CNRS UMR 7225, Paris, France, [¶]BrainPlotting, Brain and Spine Institute-ICM, Paris, France, ^{**}Fluid Team, Lyon Neurosciences Research Center, Inserm U1028, CNRS, UMR5292, University Lyon-1, Villeurbanne, France and ^{††}Service d'Anatomie et de Cytologie Pathologiques, Hôpital Lariboisière, APHP, Paris, France

Z. Csaba, T. Vitalis, C. Charriaut-Marlangue, I. Margaill, B. Coqueran, P.-L. Leger, I. Parente, A. Jacquens, L. Titomanlio, C. Constans, C. Demene, M. D. Santin, S. Lehericy, N. Perrière, F. Glacial, S. Auvin, M. Tanter, J.-F. Gherzi-Egea, H. Adle-Biassette, J.-F. Aubry, P. Gressens and P. Dournaud (2021) *Neuropathology and Applied Neurobiology* 47, 297–315

A simple novel approach for detecting blood–brain barrier permeability using GPCR internalization

Aims: Impairment of blood–brain barrier (BBB) is involved in numerous neurological diseases from developmental to aging stages. Reliable imaging of increased BBB permeability is therefore crucial for basic research and preclinical studies. Today, the analysis of extravasation of exogenous dyes is the principal method to study BBB leakage. However, these procedures are challenging to apply in pups and embryos and may appear difficult to interpret. Here we introduce a novel approach based on agonist-induced internalization of a neuronal G protein-coupled receptor widely distributed in the mammalian brain, the somatostatin receptor type 2 (SST2). **Methods:** The clinically approved SST2 agonist octreotide (1 kDa), when injected intraperitoneally does not cross an intact BBB. At sites of BBB permeability, however, OCT extravasates and induces SST2 internalization from the

neuronal membrane into perinuclear compartments. This allows an unambiguous localization of increased BBB permeability by classical immunohistochemical procedures using specific antibodies against the receptor.

Results: We first validated our approach in sensory circumventricular organs which display permissive vascular permeability. Through SST2 internalization, we next monitored BBB opening induced by magnetic resonance imaging-guided focused ultrasound in murine cerebral cortex. Finally, we proved that after intraperitoneal agonist injection in pregnant mice, SST2 receptor internalization permits analysis of BBB integrity in embryos during brain development. **Conclusions:** This approach provides an alternative and simple manner to assess BBB dysfunction and development in different physiological and pathological conditions.

Keywords: blood–brain barrier, cerebral cortex, magnetic resonance imaging (MRI)-guided focused ultrasound, neurodevelopment, neurological diseases, neurovascular unit, stroke, traumatic brain injury

Correspondence: Pascal Dournaud, Inserm NeuroDiderot U1141, Hôpital Robert Debré, 48 Boulevard Sérurier, F-75019 Paris, France. Tel: +33 (0)1 40 03 19 23; Fax: +33 (0)1 40 03 19 95; E-mail: pascal.dournaud@inserm.fr

¹These authors contributed equally to this work

Introduction

Blood–brain barrier (BBB) dysfunction is a common feature and participates in the aetiology of numerous neurological disorders in adults, including Alzheimer disease, stroke, infections, multiple sclerosis or epilepsy [1–3]. Aetiological relevance of BBB leakage is also documented in schizophrenia [4] and major depressive disorder [5,6]. In the developing brain, increasing evidence indicates that BBB disruption contributes to several paediatric neurological conditions [7–9].

The impressive growing list of neurological diseases involving BBB leakage, both in the developing and the mature brain, deserves accurate, high-resolution and technically easy *in situ* imaging methods to monitor BBB dysfunction in preclinical models. Today, microscopic examination of exogenous tracer extravasation, such as fluorescent dye-conjugated dextrans (MW 3–70 kDa) and Evans blue (MW 67 kDa when tied to albumin), remains the main way to assess functional brain microvasculature defects and maturation. Although these technical approaches have considerably improved our knowledge of BBB damage, the use of these tracers has, however, several drawbacks [10–12]. In particular, the precise delineation of regions with BBB leakage is difficult to define unambiguously, because the extent of diffusion in the brain parenchyma can vary from tracer to tracer, and autofluorescence can limit the sensitivity of the assay. More importantly, tracer injection in the blood flow of embryos (liver or heart) and young rodents requires a technically complex surgical act performed under anaesthesia [13–15].

To offer an additional technique for functional BBB assessment, we take here a different approach based on ligand-induced G protein-coupled receptor (GPCR) internalization. Our simple concept relies on the property of a brain GPCR, the somatostatin type 2 receptor (SST2), to rapidly (within minutes) internalize and concentrate in the perinuclear neuronal compartment after exogenous ligand binding before slowly (over hours) recycling [16–18]. This receptor, which is only expressed by neurons, is widely distributed in the rodent brain including the cerebral cortex, hippocampus, amygdala, striatum, septum and hypothalamus [19,20]. The SST2 appears at least as early as E11.5 in mice and remains expressed during rodent brain development [21]. At the regional level when detected by immunohistochemistry, the distribution of nonactivated receptors takes the form of a

homogeneous pattern due to localization of the SST2 at the membrane of cell bodies and dendritic arborizations. After activation by an exogenous agonist, receptors internalize and are retrogradely targeted to and concentrated in the *trans*-Golgi network (TGN) [16–18]. Such a change in receptor localization is easy to visualize and monitor, even at low microscopic magnification [22,23]. Because BBB prevents the passage to the brain parenchyma of both proteins and small molecules [24], octreotide (OCT-sandostatin-SMS-201-995; MW 1 kDa) [25], a clinically approved water-soluble agonist of this receptor, does not cross the intact BBB. We have therefore postulated that in regions where BBB permeability would be increased due to physiological or pathological conditions, SST2 agonist injected intraperitoneally would enter into the brain from the blood, reach adjacent receptors and provoke their internalization (Figure S1). The mean distance between neuronal nuclei and capillaries (15 µm) guarantees a high efficiency of diffusion-based agonist exchange between blood and neuronal membrane expressing this receptor [26]. Using complementary models, we demonstrate that this simple approach allows unambiguous characterization of brain areas where the BBB is altered in rodent adults, juveniles and embryos.

Materials and Methods

Animals

Experimental procedures were performed using Wistar rats, C57Bl/6 and OF1 mice (Charles River Laboratories, France). All efforts were made to reduce the number of animals used and any distress caused by the procedures is in accordance with the European Communities Council Directive of September 22, 2010 (2010/63/UE) and complying with ARRIVE (<https://www.nc3rs.org.uk/arrive-guidelines>) and Inserm guidelines and the ethics committees on animal experiments of Paris Diderot University.

Antibodies

The endogenous SST2 was immunolocalized using an extensively characterized rabbit monoclonal antibody (1:1000; ab134152, Abcam, Cambridge, UK) [27]. This antibody is directed towards residues 355–369 of the human SST2. This sequence is identical in mouse,

rat, and human SST2. See Supporting Information for further details.

OCT OCT (SMS 201-995; $\geq 98\%$ HPLC) was purchased from Sigma-Aldrich (St. Louis, MO, USA).

In vivo model 1: Circumventricular organs (CVOs) and arcuate nucleus of the hypothalamus (Arc)

OCT injection. Post-natal day 14 (P14) male rats ($n = 5$) were injected with OCT (2.5 mg/kg diluted in 0.01 M phosphate-buffered saline, pH 7.4 (PBS) i.p.) and were fixed 45 mins later.

In vivo model 2: Focused ultrasound-mediated non-invasive BBB disruption

BBB disruption induced by magnetic resonance imaging (MRI)-guided focused ultrasound (FUS) (MRgFUS) was performed as previously reported [28]. See Supporting Information for further details.

OCT injection. Thirty mins following BBB disruption, mice were injected with OCT (2.5 mg/kg i.p.) and were fixed 45 mins later.

In vivo model 3: Cerebral ischaemia

Ischaemia-reperfusion. Ischaemia was induced in P14 rats as previously reported [29]. See Supporting Information for further details.

OCT injection. Rats 6 h ($n = 3$), 12 h ($n = 3$) or 24 h ($n = 4$) after the ischaemia-reperfusion procedure were injected with OCT (2.5 mg/kg i.p.) and were fixed 45 mins later.

In vivo model 4: Traumatic brain injury (TBI)

Closed weight-drop head trauma. TBI was induced in P7 OF1 mice as previously described [30]. See Supporting Information for further details.

OCT injection. Mice ($n = 3$) 30 mins after the traumatic brain injury were injected with OCT (2.5 mg/kg i.p.) and were fixed 45 mins later.

In vivo model 5: Embryonic BBB permeability

OCT injection. Pregnant female C57Bl/6 mice at gestation E13.5 ($n = 3$), E14.5 ($n = 3$), E15.5 ($n = 3$) and

E18.5 ($n = 3$) were injected with OCT (2.5 mg/kg i.p.) and were fixed 45 mins later.

Tissue preparation for in vivo models 1-5

Adult mice and post-natal day 14 (P14) male rats. Forty-five mins after OCT injection, animals were deeply anaesthetized with sodium pentobarbital (150 mg/kg i.p.; Ceva Sante Animal, Libourne, France) and perfused through the ascending aorta with 100 mL of 4% paraformaldehyde (PFA) in 0.1 M phosphate buffer, pH 7.4 (PB). Brains were dissected, post-fixed in the same fixative overnight at 4°C, cryoprotected, frozen in liquid isopentane at -45°C and sectioned in the coronal plane at a thickness of 30 μm and collected in PBS.

Pregnant female mice and embryos. Forty-five mins after OCT injection, dams were deeply anaesthetized with sodium pentobarbital (150 mg/kg i.p.), and embryos were dissected and fixed in 4% PFA in PB overnight at 4°C. The brains of the embryos ($n = 5$ per age) were cut in the coronal plane on a vibratome at 60 μm and collected in PBS. Additional whole embryos at E15.5 ($n = 3$) were cut in the sagittal plane to analyse the distribution of SST2 in the pancreas. In parallel, dams were perfused, their brains were post-fixed, cryoprotected and sectioned as described above.

In vitro model: OCT transport assays through Human Primary Brain Microvascular Endothelial Cell (hPBMEC) monolayers

The hPBMECs were cultured as previously described [31]. See Supporting Information for further details. Differentiated hPBMECs with the BBB phenotype ($\text{TEER} > 1000 \Omega\text{cm}^2$) were treated or not with 1 M mannitol in serum-free culture medium for 30 min to temporarily open tight junctions. Then, mannitol solution was removed and replaced by culture medium. Tight junction opening was evaluated with the measurements of fluorescein permeability, a small hydrophilic compound known to cross the BBB via the paracellular route. In both mannitol-treated and untreated hPBMECs monolayers, OCT at 10 μM or 100 μM concentration was added to the luminal compartment. The medium of the abluminal compartment was then collected during a 2-hour period ($n = 3$ per condition).

To analyse the passage of OCT across the hPBMECs monolayer, the medium collected from the abluminal

compartment was then applied to DAOY medulloblastoma cells, which endogenously express SST2. The agonist-induced SST2 internalization was monitored after cell fixation. DAOY cells were grown in DMEM with 1 g/L D-Glucose, L-Glutamine and Pyruvate (31885-023; Gibco, Life Technologies, Carlsbad, CA, USA) containing 10% foetal bovine serum (FBS; Invitrogen, Life Technologies) and 5000 IU/mL Penicillin/Streptomycin (Invitrogen, Life Technologies). Cells were incubated for 20 min at 37°C with either 1 µM OCT or medium collected from the abluminal compartment of hPBMECs with or without mannitol pre-treatment. At the end of the incubation period, DAOY cells were fixed with 4% PFA supplemented with 4% sucrose in PB for 20 min at room temperature (RT).

Immunocytochemistry

The SST2 receptor was immunolocalized on brain sections (*in vivo* models 1-5), whole embryo sections (*in vivo* model 5) and DAOY cells (*in vitro* model). Brain sections were selected at the level of the circumventricular organs (*in vivo* model 1), at the level of the focused ultrasound-mediated BBB opening (*in vivo* model 2), at the level of the ischaemia-reperfusion lesions (*in vivo* model 3), at the level of the traumatic brain injury (*in vivo* model 4) and at the level of the caudal embryonic cortex (*in vivo* model 5). See Supporting Information for further details.

Confocal microscopy Immunofluorescent sections from all *in vivo* and *in vitro* models were analysed using a Leica TCS SP8 confocal scanning system (Leica Microsystems, Wetzlar, Germany) equipped with 405-nm Diode, 488-nm Ar, 561-nm DPSS and 633-nm HeNe lasers. See Supporting Information for further details.

Stereological analysis Stereological measures of estimated volume in the *in vivo* model 2 was performed with the Volumest plug-in [32] in the Fiji distribution of ImageJ [33]. Brightfield images of serial coronal sections separated by 180 µm were collected. The number of serial sections, the thickness of the sections, the sampling interval and pixel-to-µm scaling were entered into the Volumest plug-in. Next, the cortical areas displaying BBB disruption detected by SST2 internalization were manually traced and the volume estimate was calculated in the Volumest plug-in [32].

Electron microscopy Pre-embedding immunogold immunocytochemistry of SST2 in adult C57Bl/6 mice was performed as previously reported [32]. See Supporting Information for further details.

Results

Sensory CVOs

The sensory CVOs, including the subfornical organ (SFO), organum vasculosum of the lamina terminalis (OVLT), and area postrema (AP) (Figure 1a), receive blood supply through branches of the anterior cerebral (OVLT and SFO) and of the cerebellar (AP) arteries. Sensory CVOs consist of numerous capillary loops that have size-dependent and function-related permissive vascular permeability due to the fenestrated nature of their endothelial lining. They allow direct exchange between the blood and the adjacent CNS parenchyma and are critical regulators of cardiovascular function, body fluid balance, immune signalling, temperature control, appetite and reproduction [34].

Because sensory CVOs are unique areas of the brain where capillaries are permeable, we first tested our working hypothesis in the AP and OVLT, two sensory CVOs in which neurons natively express the SST2. Rats received a single intraperitoneal (i.p.) injection of PBS or OCT (2.5 mg/kg) and were perfused 45 mins after. This dose and time-point was chosen on the basis of our previous studies and preliminary experiments to allow complete internalization and targeting of activated receptors to the TGN [16-18]. At low magnification, SST2 immunoreactivity appeared to fill the entire AP and OVLT nuclei in control animals (Figure 1b,h). At higher magnification, serial optical sections using confocal microscopy revealed a meshwork of labelled dendrites and neuronal cell bodies (Figure 1c,i). In both structures, receptor immunoreactivity was predominantly localized at the dendritic and perikaryal plasma membrane (Figure 1d,j), characteristic of nonactivated receptors. In OCT-injected animals, the homogeneous immunostaining pattern was no longer apparent and neuronal cell bodies with clustered pattern of immunoreactivity were evident (Figure 1e,f,k,l). At high magnification, immunoreactivity was confined to intracytoplasmic granules near the nucleus and in proximal dendrites (Figure 1g,m), a characteristic configuration of activated and internalized receptors.

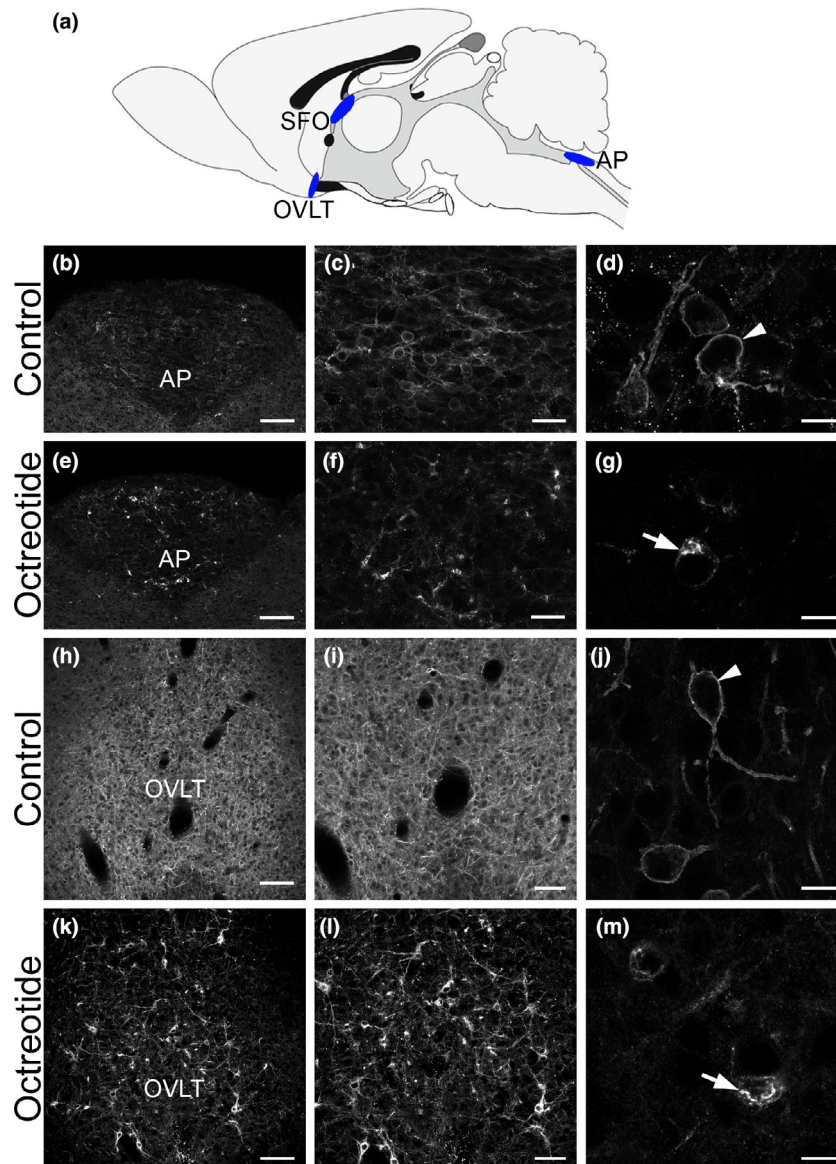


Figure 1. Detection of capillary permeability in sensory circumventricular organs (CVOs): area postrema (AP) and organum vasculosum of the lamina terminalis (OVLT). Schematic localization of CVOs in the rat brain (a). At low microscopic magnification, somatostatin receptor 2 (SST2) immunoreactivity appears to fill the entire AP (b) and OVLT (h) of control rats. Higher magnification reveals a meshwork of labelled dendrites and neuronal cell bodies (c, i). At high magnification, SST2 immunoreactivity is localized at the cell surface of neurons in the form of a fluorescent ring both in the AP (d) and OVLT (j) (arrowheads) and in a network of dendritic processes. Forty-five minutes after i.p. injection of SST2 agonist octreotide, a dramatic change of SST2-immunoreactive pattern can be observed. At the regional level, the homogenous SST2 labelling is no longer evident, SST2 immunoreactivity is concentrated in somatodendritic profiles in the AP (e, f) and OVLT (k, l). At the cellular level, SST2 immunoreactivity is confined to bright fluorescent granules in the cytoplasm of neurons in the AP (g) and OVLT (m) (arrows), characteristic of agonist-induced receptor internalization. SFO, subfornical organ. Scale bars: b, e, h, k, 100 μ m; c, f, 30 μ m; i, l, 60 μ m; d, g, j, m, 10 μ m.

Importantly, in OCT-injected animals, changes in receptor-immunoreactive patterns were never observed in regions inside the BBB and adjacent to CVOs such as the nuclei of the horizontal and vertical limb of the diagonal band of Broca (adjacent to OVLT) and nucleus

of the solitary tract (adjacent to AP), or distant from CVOs such as the locus coeruleus, the cerebral cortex (Figure 2g-l) or the hippocampus. These first studies clearly demonstrated that OCT injected in the periphery reached the brain parenchyma only in regions where

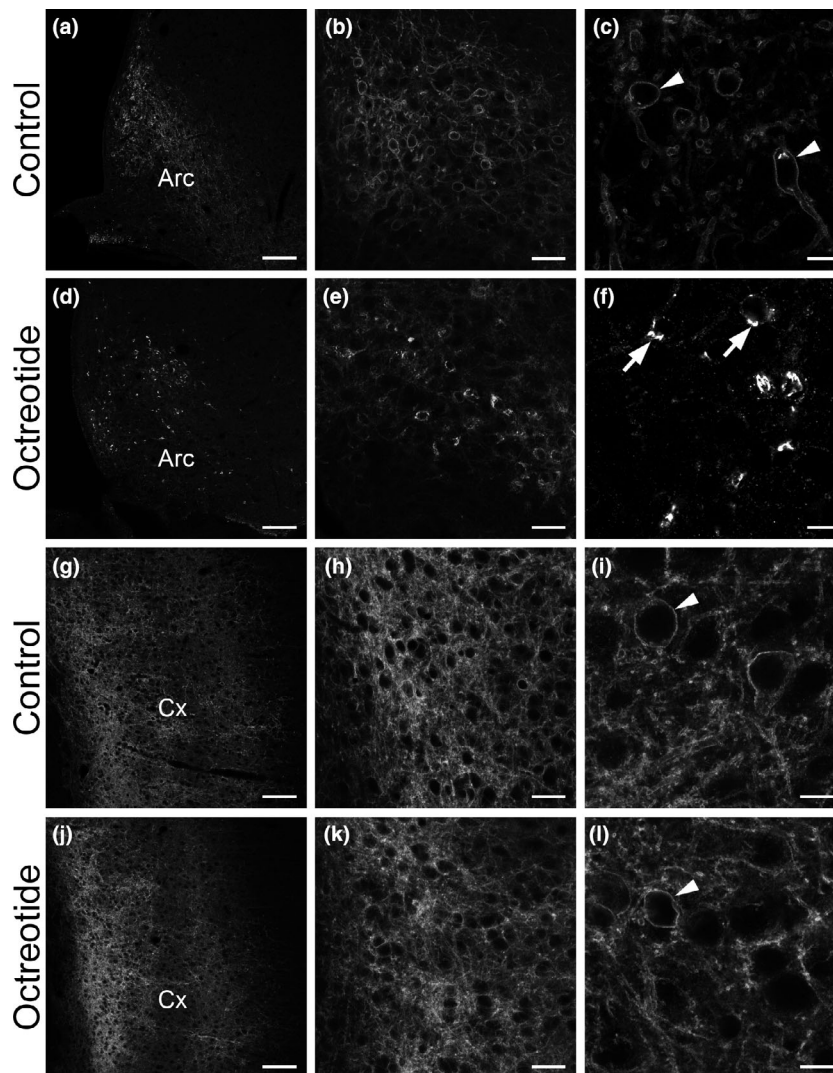


Figure 2. Detection of blood–brain barrier (BBB) permeability in the hypothalamic arcuate nucleus (Arc). At low microscopic magnification, the somatostatin receptor 2 (SST2) immunoreactivity appears to fill the Arc (a) and cerebral cortex (Cx; g) in control rats. Higher magnification reveals a meshwork of labelled dendrites and neuronal cell bodies (b, h). At high magnification, SST2 immunoreactivity is localized at the cell surface of neurons in a form of a fluorescent ring both in the Arc (c) and Cx (i) (arrowheads) and in a meshwork of dendrites. Forty-five minutes after i.p. injection of SST2 agonist octreotide (OCT), a change of the SST2 immunoreactive pattern in the Arc can be observed. At low magnification, the homogenous SST2-immunoreactive pattern is no longer evident and the receptor immunoreactivity is concentrated in somatodendritic profiles (d, e). At high magnification, SST2 immunoreactivity is confined to bright fluorescent granules in the cytoplasm of Arc neurons (f) (arrows), characteristic of agonist-induced receptor internalization. By contrast, in the Cx, OCT treatment has no effect on SST2-immunolabelling at the regional (j, k) or cellular (l) levels (arrowhead). Scale bars: a, d, g, j, 100 µm; b, e, h, k, 30 µm; c, f, i, l, 10 µm.

capillaries were permeable to a 1 k-Da molecule and induced efficient internalization of the SST2.

Arcuate nucleus of the hypothalamus

The Arc display several populations of neurons that are pivotal for regulating energy homeostasis, food intake

and cardiovascular functions. Because of this central role at the interface between the brain and the periphery, a few studies have hypothesized that the Arc could share common features with classical CVOs [35,36]. This issue is, however, still a matter of debate awaiting clear-cut demonstration. We have therefore reinvestigated this subject using our approach. Following OCT

injection, we observed the same results as in the AP and OVLT. Membrane-associated SST2 in Arc neurons internalized and clustered in TGN-like structures (**Figure 2a–f**). In a previous study using Evans blue, the dye extravasated only in the Arc of 24-hour fasted mice but not in control-fed mice [37], whereas our results unambiguously establish that Arc vascular circulation was permeable to at least 1 kDa molecules in naïve animals. This suggests a higher sensitivity of our approach in comparison to Evans blue dye diffusion. Our results thus open the intriguing possibility of a direct passage from blood to Arc neurons of small peptides [38,39] or cytokines [40].

Focused ultrasound-mediated noninvasive BBB disruption

Efficient drug delivery across the BBB into the brain parenchyma remains a major challenge to treating central nervous system disorders for both academic research and the pharmaceutical industry. FUS has recently gained attention for its potential application as a method for locally and transiently disrupting the BBB and thereby facilitating drug delivery into the brain parenchyma [41,42]. Having demonstrated that we can easily detect brain areas in which BBB was physiologically open, we next investigated whether our technical approach would reveal BBB disruption induced by MRgFUS. We targeted primarily the cerebral cortex, a region with many SST2-expressing neurons. The highest intensities of SST2 immunolabelling are found in layers 5 and 6, while layers 2 to 4 are less intensely labelled. Using our MRgFUS setup, T1-weighted (T1w) MRI images demonstrated gadolinium (Gd) extravasation after microbubble sonication of the targeted area. Extravasation was evident from the cerebral cortex to deep brain structures (**Figure 3a–d**). There was no visible evidence of haematoma formation or other obvious deleterious consequences of MRgFUS on either MRI studies performed after the BBB disruption or in any of the histological studies. Receptor immunohistochemical staining demonstrated that in the area displaying Gd extravasation on MRI images such as the cerebral cortex dorsally or the amygdala ventrally, SST2 internalization was manifest following peripheral OCT injection (**Figure 3e,f,h,i**; Videos S1–2), as previously observed in CVOs and Arc. Clear-cut borders between areas of internalization and areas where internalization did not

occur were evident (**Figure 3e**). It was therefore easy to estimate the volume of BBB disruption in the deep cortical layers using serial sections ($3.59 \times 10^9 \mu\text{m}^3$; animal 3) (**Figure S2**). On the contralateral side of the MRgFUS-targeted region, as well as in other brain areas inside the BBB, SST2 internalization was never observed (**Figure 3g,j,k**). Of note, we did not observe any change in SST2 distribution or expression at the regional or cellular levels in the brain of PBS-injected animals following the MRgFUS procedure. Together, these results clearly indicate that a comprehensive mapping of MRgFUS-BBB opening was possible, thanks to extravasation of the receptor agonist OCT, confirming our expectations. In support of *in vivo* Gd extravasation, it should help to better define at the cellular level the optimum MRgFUS parameters (acoustic pressure, frequency of the transducer, pulse repetition frequency, microbubble size, pulse length) that allow safe, efficient and selective BBB disruption. Testing MRgFUS for BBB opening in larger animal species is a prerequisite for transferring the procedure to human trials. In this context, our approach is also pertinent since the SST2 is expressed in the brain of nonhuman primates and larger animal species [43]. Of note, because the SST2 display both anti-proliferative and anti-epileptic properties [43], our MRgFUS noninvasive approach could also be of particular interest to test the therapeutic values of SST2 agonists in preclinical models of brain tumours and epilepsy.

Cerebral ischaemia

Arterial ischaemic stroke is increasingly recognized as a serious paediatric problem. Groups at risk are newborns (the first 28 days of life), especially full-term infants and older children with sickle cell anaemia or congenital heart defects [44]. Neonatal stroke produces significant morbidity and severe long-term neurological and cognitive deficits, including cerebral palsy, epilepsy, neurodevelopmental disabilities, impaired vision and language function and emotional symptoms. There is a large body of work demonstrating disturbances of BBB function following hypoxia and/or ischaemia in adult animal models [45]. Surprisingly, very few studies focused on the developing brain, at least in part due to some difficulties of accurately assessing BBB integrity in pups using available technical approaches. Because some [46–48], but not all

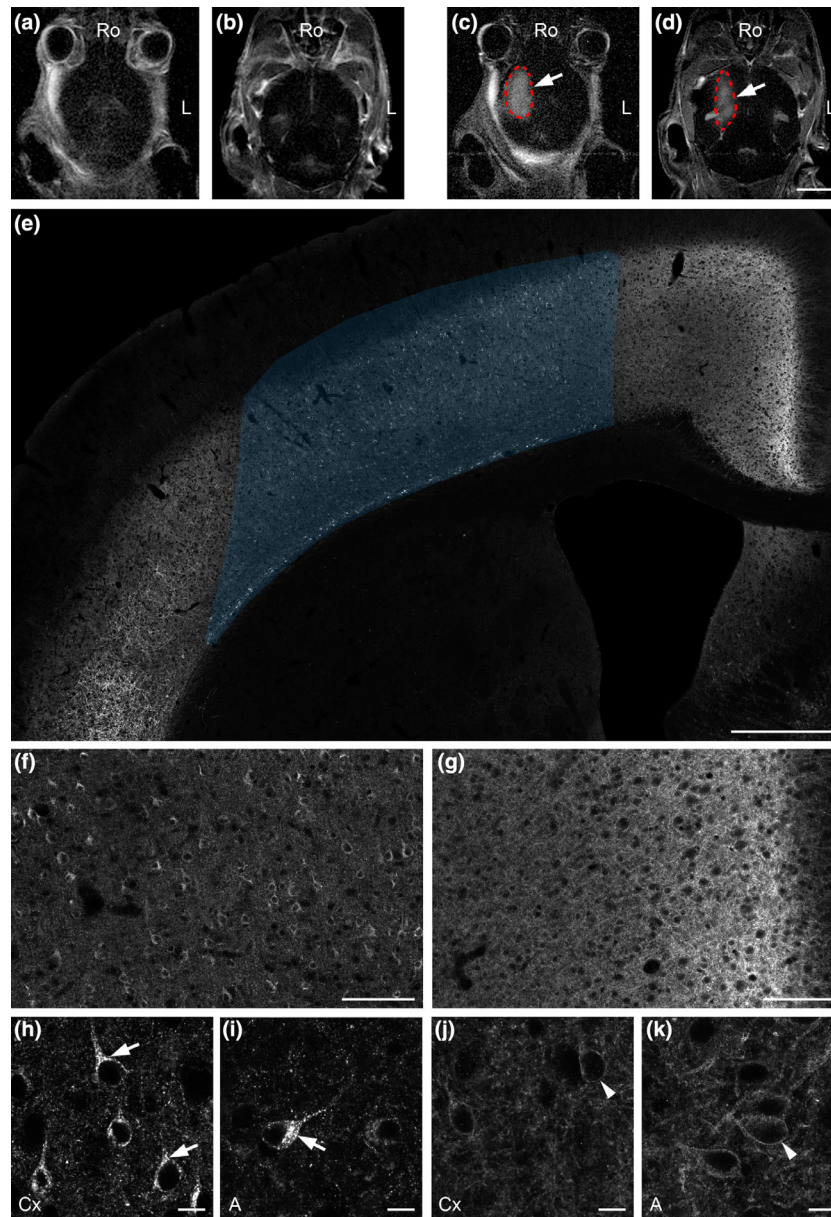


Figure 3. Detection of somatostatin receptor 2 (SST2) agonist extravasation after focused ultrasound-mediated (MRgFUS) disruption of the blood–brain barrier (BBB) in the mouse brain. Control T1-weighted MR images close to the dorsal surface (a) and in deep brain areas (b) obtained before microbubble injection. The gadolinium (Gd)-based contrast enhancement in the FUS-targeted area (c, d; red dotted lines) demonstrates opening of the BBB by microbubble sonication (arrows), which extends from dorsal (c) to ventral (d) brain areas. In the FUS-targeted right cerebral cortex, clear-cut area of agonist-induced SST2 internalization is detected 45 minutes after i.p. injection of SST2 agonist octreotide (shaded area on e). Magnified panels show somatodendritic SST2 immunoreactivity in the FUS-targeted cortex (f) as compared to the homogenous SST2 labelling in the surrounding cortex (g). At high magnification, agonist-induced SST2 internalization within the FUS-targeted area is evidenced by the bright immunofluorescent granules in the cytoplasm (arrows) dorsally in the cortex (Cx; h) and ventrally in the amygdala (A; i). On the control side, SST2 is located at the surface of neurons both in the Cx (j) and in the A (k) (arrowheads). Ro, rostral; L, lateral. Scale bars: a–d, 4 mm; e, 500 μ m; f, g, 100 μ m; h–k, 10 μ m.

[15], of these studies do indicate that barrier function is disturbed during ischaemic insults in neonates and juveniles, we investigated whether our methodological

approach could reveal BBB leakage in a P14 rat ischaemic model. At 24 h after the initial insult, peripheral OCT injection induced large areas of SST2

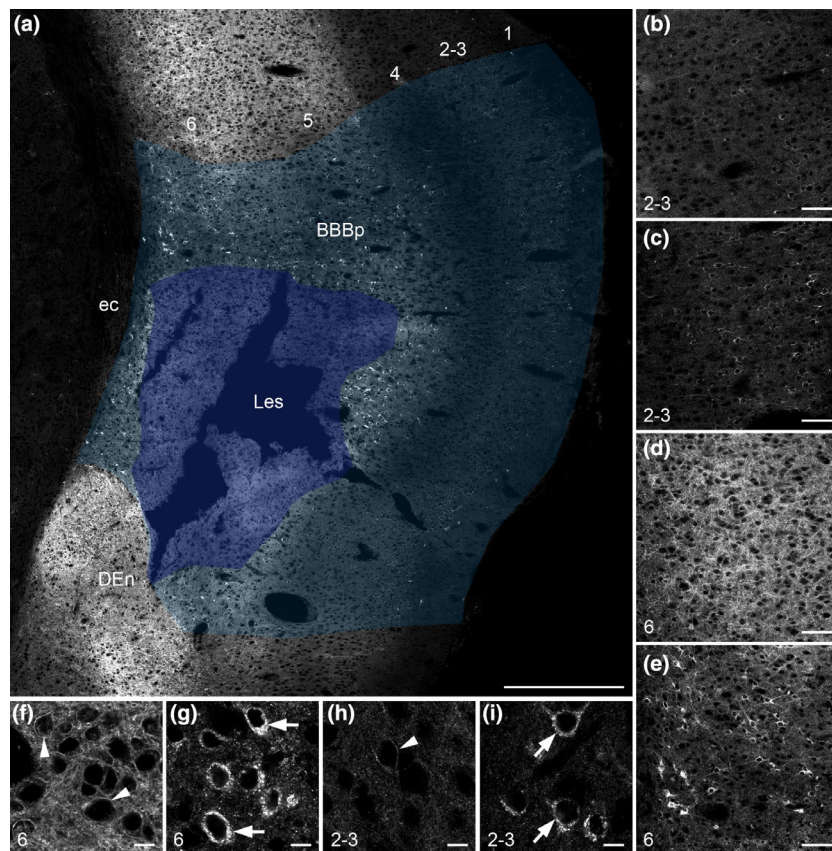


Figure 4. Detection of blood–brain barrier (BBB) permeability in a juvenile cerebral ischaemia rat model. Twenty-four hours after the cerebral ischaemia, agonist-induced somatostatin receptor 2 (SST2) internalization is detected in the area of pathological BBB permeability (BBBp; light shaded area on a) around the necrotic cortical lesion (Les; dark shaded area on a) 45 minutes after i.p. injection of SST2 agonist octreotide. Magnified panels show somatodendritic SST2 immunoreactivity in the BBBp both in the superficial cortical layers 2–3 (c) and in the deep cortical layer 6 (e) as compared to the homogenous SST2 labelling surrounding the BBBp in layers 2–3 (b) and 6 (d). Note that SST2 internalization is evident in both layers 2–3 and 5–6, although the intensity of immunoreactivity is relatively low in the superficial layers as compared to the deep ones. At high microscopic magnification from the BBBp, layer 2–3 (i) and layer 6 (g) neurons are characterized by the bright intracytoplasmic granules (arrows) as compared to the surface labelling of neurons in layers 2–3 (h) and layer 6 (f) in the intact cortex. DEn, dorsal endopiriform nucleus; ec, external capsule. Scale bars: a, 500 μ m; b–e, 100 μ m; f–i, 10 μ m.

internalization around the core of the cortical lesion (Figure 4a). Neurons expressing internalized receptors were visible in cortical layer 2–layer 6, in accordance with the fact that the core of the infarct is located in deep and mediocortical layers [49] (Figure 4b–i). Again, rapid examination of the sections allowed easy differentiation between regions where internalization occurred and regions where internalization did not. We next monitored the cortical neurons expressing internalized receptors, 6, 12 and 24 h after stroke in comparable areas adjacent to the core of the lesion. Although few neurons with internalized receptors were visible at 6 h after stroke (Figure 5a), the area

containing neurons with internalized SST2 became progressively wider (Figure 5b,c). Such a result strongly suggests that areas of receptor internalization are not due to passive diffusion of OCT within the brain parenchyma but represent time-dependent BBB disruption after the ischaemic insult. Of note, we did not observe any change in SST2 distribution or expression at the regional or cellular levels in PBS-injected ischaemic animals, except for a loss of receptor immunoreactivity in the necrotic core due to neuronal cell death. Our approach is therefore appropriate to easily and accurately monitor damage of the BBB in adult but also in juvenile ischaemic stroke models.

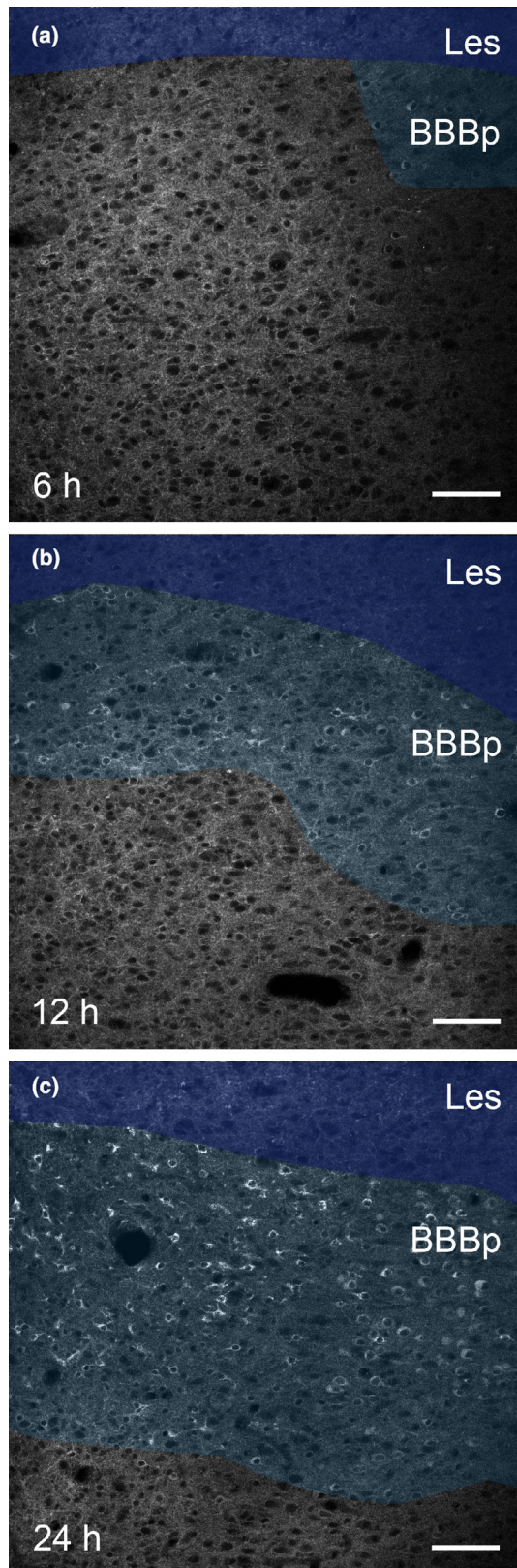


Figure 5. Change of blood–brain barrier (BBB) permeability in a juvenile cerebral ischaemia rat model. Extravasation of i.p. injected somatostatin receptor 2 (SST2) agonist octreotide was monitored 6 h (a), 12 h (b) and 24 h (c) after the initial cerebral ischaemia. Six hours after the cerebral ischaemia, only few neurons with internalized SST2 are detected in the area of pathological BBB permeability (BBBp; light shaded area on a) adjacent to the necrotic cortical lesion (Les; dark shaded area on a). Twelve hours after the cerebral ischaemia, a larger number of neurons with internalized SST2 are localized in a narrow band (light shaded area on b) around the cortical lesion (dark shaded area on b). The BBBp with neurons of internalized SST2 becomes wider 24 h after the cerebral ischaemia (light shaded area on c) around the cortical lesion (dark shaded area on c). Scale bars: a–c, 100 μ m.

Traumatic brain injury

The consequences of head trauma are also a serious paediatric problem [50]. Deciphering the pathophysiology of the increased susceptibility of the immature brain is therefore of critical importance. Moreover, children under 4 years of age suffer TBI more often than any other age group. Despite its paediatric importance, the accurate assessment of BBB integrity following head injury, which was widely studied in adult animal models [51], is lacking in pups, at least partly because of technical difficulties with available approaches. Because our approach is particularly suitable in pups, we studied whether BBB disruption following TBI could be detected in mouse pups. Thirty minutes after TBI, SST2 internalization was evident only in a limited number of neurons following systemic OCT administration. They were localized on the left side at the rostrocaudal level of the contusion impact (**Figure 6a**) in the dentate gyrus, subiculum (**Figure 6e–g**) and retrosplenial cortex (**Figure 6k–m**). The dorsal cortical areas directly beneath the skull at the level of the impact did not display agonist-induced SST2 internalization. On the contralateral side of the TBI, SST2 internalization was never observed (**Figure 6b–d,h–j**). These results demonstrate for the first time that TBI induces early BBB alterations in particular regions of the juvenile brain, opening the way to detailed analyses of the short- and long-term consequences of such alterations, including inflammation, neuronal cell death or connectivity.

Cellular and subcellular localization of SST2 in the murine brain

Double-labelling experiments at the light microscopic level confirmed that SST2s are internalized only in

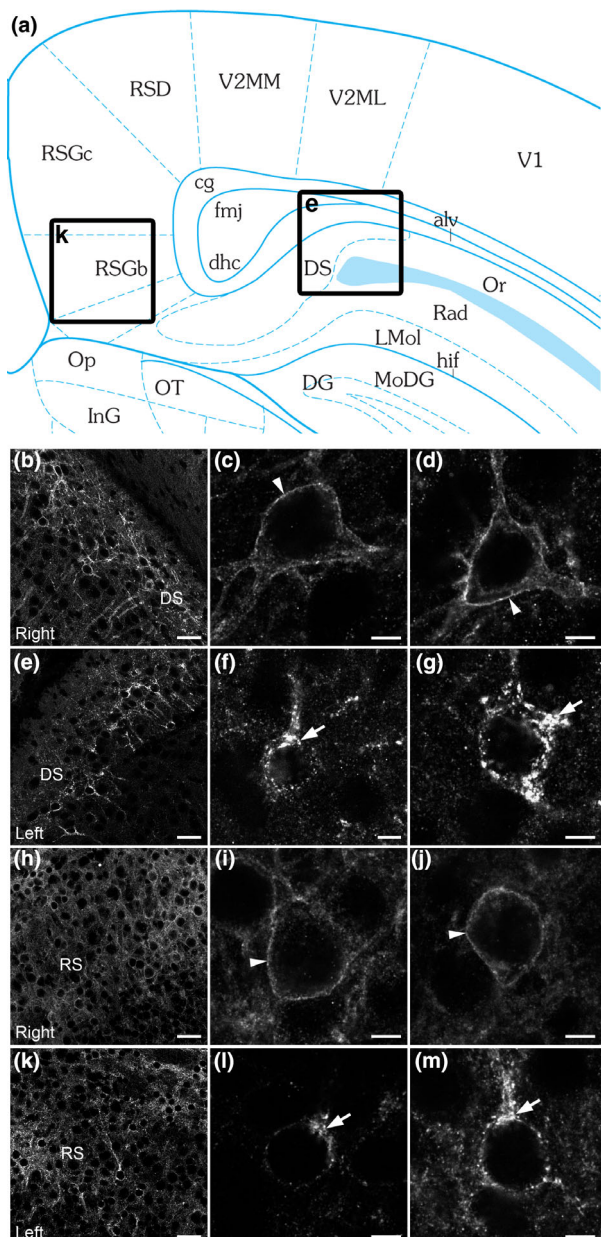


Figure 6. Detection of blood–brain barrier (BBB) permeability in a juvenile traumatic brain injury (TBI) model. Schematic of the mouse brain regions at the level of the contusion impact (a). Thirty minutes after the TBI, agonist-induced somatostatin receptor 2 (SST2) internalization is detected in neurons of the dorsal subiculum (DS; e) and retrosplenial cortex (RS; k). At high microscopic magnification, neurons are characterized by the bright intracytoplasmic granules in the DS (f, g) and RS (l, m) (arrows) 45 min after i.p. injection of SST2 agonist octreotide. On the contralateral side of the contusion, by contrast, the SST2 immunoreactivity is homogeneously distributed in the DS (b) and RS (h). At high magnification, SST2 immunoreactivity is localized at the cell surface of neurons in the DS (c, d) and RS (i, j) (arrowheads). Scale bars: b, e, h, k, 30 μ m; c, d, f, g, i, j, l, m, 5 μ m.

neurons but not in astrocytes, microglial cells or endothelial cells (Figures S3, S4a–c). Moreover, pre-embedding immunogold immunocytochemistry demonstrated at the ultrastructural level that SST2 immunoparticles were associated with neuronal perikarya and dendrites. In agreement with the C-terminal epitope of the antibody, SST2 immunoparticles were localized at the plasma membrane outlining the internal side (Figure S4d–f) or in endosomes outlining the external side (Figure S4g). It is of note that neither glial nor endothelial cells displayed any SST2 immunogold staining (Figure S4d–g) in agreement with previous studies [16,17,53].

Embryonic BBB permeability

From a clinical point of view, it is of particular importance to understand the physiological properties of the BBB during normal and pathological development. On the one hand, such knowledge would help better understand whether and how drugs and toxins entering the foetal circulation from the mother would impact the developing brain. On the other hand, BBB disruption could provide therapeutic windows to deliver neuroprotective molecules in the context of early brain insults. Although molecular and mechanistic insights of BBB development is gradually being discovered [2,52], the developmental regulation of BBB permeability still represents a major issue. To our knowledge, only few studies have recently set up this challenge and identified the role of key molecular players in functional BBB maturation, *Mfsd2a* [14] and *LSR/angulin-1* [13]. In the former, a 1–5 μ l solution of lysine fixable 10 kDa dextran-tetramethylrhodamine (TRITC) was injected in the liver of embryos (E13.5 to E15.5) still attached via the umbilical cord to the anaesthetized dams. In the latter, after caesarean section of anaesthetized pregnant females, embryos (E13.5 to E16.5) dissected out from yolk sacs, but still attached to the placenta, were injected into the heart with a solution of 6 μ l TRITC-conjugated 10 kDa dextran or Sulfo-NHS-biotin. Both studies, in agreement with pioneer studies by Daneman and colleagues [54], concluded that dyes stop leaking in the cerebral cortex between E14.5 [13] and E15.5 [14]. Clinical studies have reported transplacental passage of OCT by passive diffusion without detectable modification during the maternal–foetal transfer, nor adverse effects to the foetus

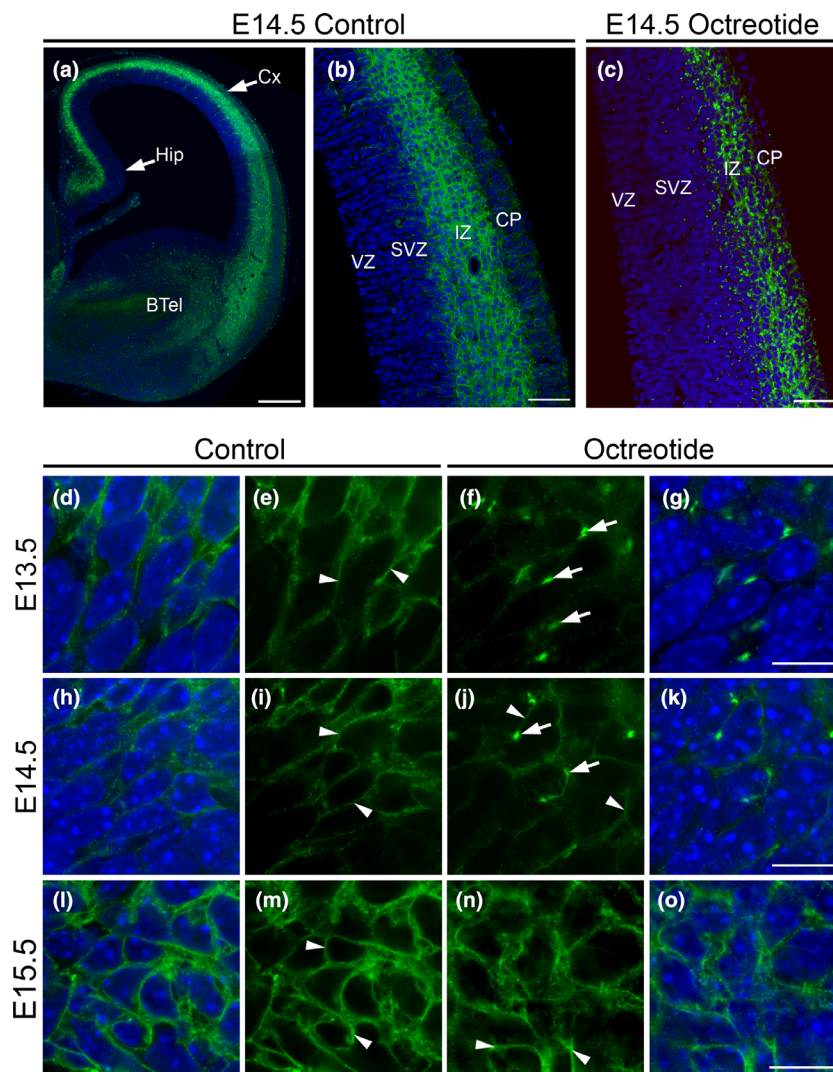


Figure 7. Analysis of blood–brain barrier (BBB) permeability in E13.5–E15.5 embryos. In a coronal section of an E14.5 control embryo, somatostatin receptor 2 (SST2) immunoreactivity is localized in the hippocampus (Hip), cerebral cortex (Cx) and in the basal telencephalon (BTel) (a). In the Cx of controls, a meshwork of SST2 immunolabelling is intense in the intermediate zone (IZ) and weak in the cortical plate (CP). Few SST2-immunolabelled radial processes are also detected in the ventricular zone (VZ) and subventricular zone (SVZ) (b). In an E14.5 embryo of an octreotide (OCT)-treated dam, the SST2-immunoreactive pattern is drastically modified and appears as intense immunoreactive puncta in the IZ and CP (c). At high microscopic magnifications from the IZ of E13.5 (d, e), E14.5 (h, i) and E15.5 (l, m) control embryos, SST2 immunolabelling is at the cell surface of neurons and in a network of neuritic processes (arrowheads). By contrast, in an E13.5 embryo of an OCT-treated dam (f, g), SST2-immunostaining in the IZ is confined to bright fluorescent granules in the perinuclear compartment (arrows), characteristic of agonist-induced receptor internalization. Note that in an E14.5 embryo of an OCT-treated dam (j, k), the SST2 immunolabelling in the IZ is partly intracellular (arrows) but also at the cell surface (arrowheads). In an E15.5 embryo of an OCT-treated dam (n, o), SST2 immunoreactivity in the IZ is predominantly localized at the cell surface (arrowheads) similarly to controls. Nuclei are labelled with DAPI. Scale bars: a, 350 μ m; b, c, 65 μ m; d–o, 10 μ m.

[55,56]. Because SST2 appears at least as early as E11.5 in mice and remains expressed during rodent brain development (Figure 7a–c) [21], we investigated whether i.p. OCT injection in pregnant dams can reveal dynamics of BBB maturation in E13.5 to E18.5

embryos. OCT injection of pregnant females indeed induced a massive redistribution of the receptor from the membrane to intracellular compartments in the cortex of E13.5 embryos (Figure 7d–g). At E14.5, internalization was still clearly visible although in contrast

to earlier ages, membrane-associated receptors were present (Figure 7a-c,h-k). At E15.5 and after, while SST2 internalization was observed in the periphery such as in the pancreas (Figure S5), it was no longer observed in the cerebral cortex (Figure 7l-o) demonstrating that BBB was sealed to molecules > 1 kDa, in agreement with the studies discussed above. Together, our results demonstrated that this simple approach, which avoids dam anaesthesia, caesarean section and embryo manipulation, allowed the spatial and temporal monitoring of functional BBB maturation across brain development. It should also help to analyse the consequences of different maternal health status (i.e. infectious, nutritional, toxicologic) and genetic manipulations of key proteins of BBB integrity and maturation.

In vitro octreotide transport assay through hPBMECs

Although OCT does not cross an intact BBB, previous studies have demonstrated that OCT or somatostatin analogues can cross the endothelial monolayer via the paracellular route when tight junctions become loose [57–59]. This is in accordance with our results obtained by MRgFUS-BBB opening. This method utilizes

the mechanical effect of microbubble oscillations which induced a transient disruption or loosening of the tight junctions in the brain endothelial cells thus facilitating paracellular permeability [41]. In addition, we have conducted experiments using an *in vitro* model of adult human BBB to monitor passage of OCT through the brain endothelial monolayer by agonist-induced receptor internalization. Using a hypertonic concentration of mannitol, we induced a rapid and reversible increase in hPBMECs permeability to small hydrophilic molecules through the alteration of tight junction complexes [60]. As control, TEER drastically fell with Mannitol treatment ($< 20 \Omega\text{cm}^2$), and the functionality of the tight junctions was measured in each insert: with the treatment of mannitol, the fluorescein permeability showed an increase of $600 \pm 25\%$ ($0.135 \times 10^{-3} \text{ cm/min}$ in basal conditions). We assessed permeability of 10 and 100 μM OCT from the luminal side to the abluminal side in control conditions vs. after mannitol treatment. After an incubation of 2 h, abluminal media was collected and applied to DAOY cells that endogenously express the SST2 receptor. In control conditions, the distribution of SST2 in DAOY cells was restricted to the cell membrane (Figure 8a-c). By contrast, incubation of the abluminal media obtained following mannitol pretreatment induced a massive internalization of SST2 in

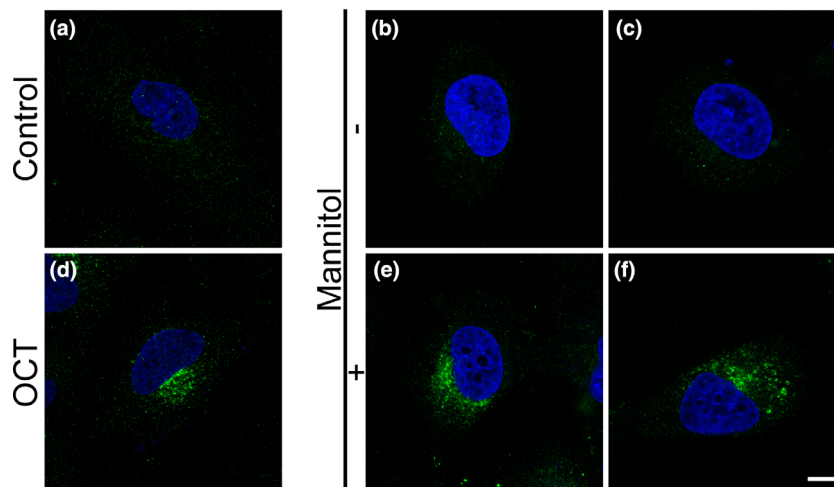


Figure 8. Detection of octreotide transport through Human Primary Brain Microvascular Endothelial Cells (hPBMECs). In a control DAOY cell, somatostatin receptor 2 (SST2) immunoreactivity is evenly distributed over the cellular surface (a). Similarly, SST2 immunoreactivity in cells treated for 20 mins with the abluminal medium of hPBMECs without mannitol pretreatment is also evenly distributed on the surface, with both 10 μM (b) or 100 μM (c) luminal octreotide (OCT) concentrations. Treatment with 1 μM OCT for 20 mins results in a massive redistribution of SST2 immunoreactivity into bright fluorescent intracytoplasmic granules (d). Similarly, SST2 immunoreactivity in cells treated for 20 mins with the abluminal medium of hPBMECs following mannitol pretreatment is also confined to bright fluorescent granules, with both 10 μM (e) or 100 μM (f) luminal OCT concentrations. Nuclei are labelled with DAPI. Scale bars: a–f, 10 μm .

DAOY cells (Figure 8d-f). Taken together, these results indicate that OCT crosses the endothelial cell monolayer by paracellular transport only when tight junctions are widened.

Discussion

BBB dysfunction is increasingly recognized as being part of the aetiological processes that drive a wide range of neurological disorders. Reliable and reproducible approaches are therefore mandatory to accurately monitor BBB disruption in animal models. Visualization of BBB permeability is classically performed using injection of Evans blue or labelled dyes into the blood flow [10-12,61]. However, modes of injection require trained and skilled personnel and are challenging to establish in pups and embryos. Animal perfusion as well as brain tissue manipulation have to be carefully monitored to ensure reliable interpretation.

In the present study, we propose and assess a novel alternative method for rapid and precise evaluation of animal BBB disruption and development. The major strength of this method is that a single intraperitoneal injection of a somatostatin analogue (octreotide) induces an easily detectable receptor internalization restricted to the region of BBB leakage.

Redistribution of SST2 labelling

After agonist binding, membrane-associated SST2s internalize and concentrate in the perinuclear neuronal compartment [16-18]. Such a process avoids any concern relating to the detection of dye extravasation. In the different models we have analysed, the clear-cut difference between neurons that internalized the SST2s and those which did not circumvent any misleading interpretation. SST2 receptor targeting to the TGN after internalization is only observed at pharmacological doses. Such doses induce an acute and massive receptor activation that synchronizes internalization, trafficking and targeting of the receptors to the TGN. After physiological or pathophysiological activation by endogenous ligand, only a few vesicles resembling endosomes bearing SST2 receptor can be visualized in dendrites and/or the neuronal cytoplasm [16,17]. Such labelling cannot be confused with the massive localization of the receptors in the TGN induced by an exogenous ligand. In addition, because of the high densities

of neurons expressing this receptor, delineation of the area with BBB leakage with our method is highly accurate.

Animal and tissue manipulations

Another key advantage of this approach concerns animal and brain tissue manipulation. In contrast to classical dye injection methods, the receptor agonist injections are done intraperitoneally. This limits animal stress associated with experimental procedures and avoids anaesthesia which can be source of changes in BBB permeability [62]. Such a route of injection is particularly beneficial for BBB studies in pups. Because of the transplacental passage of OCT, this method also offers a simple way to study BBB in embryos.

Detection of BBB leakage

Detection of BBB leakage through SST2 internalization is realized by classical immunohistochemical procedures, which are routinely performed in research laboratories, and excellent antibodies are commercially available. Neither perfusion of the animals nor brain tissue manipulation can influence the pattern of receptor localization. The clear-cut identification of BBB leakage by standard immunohistological procedures makes quantification simple and accurate. The regional and cellular distribution of this somatostatin receptor have been indeed particularly documented [16-18]. In addition, because SST2 detection is compatible with both paraformaldehyde and glutaraldehyde fixations, co-localization of different proteins of interest at the BBB, by light or electron microscopy, can be realized in the same brain samples. Of note, the SST2 is not only present in the rodent brain but also in larger mammal species including primates [63-65]. Our approach is therefore suitable to study BBB integrity in different clinically relevant experimental models.

Advantages of the SST2 agonist

To induce SST2 internalization we chose the commercially available SST2 agonist OCT, which display nM affinity range for this receptor. OCT is a cyclic octapeptide which was approved by the US Food and Drug Administration (FDA) in October 1988 for treatment of acromegaly, treatment of diarrhoea and flushing in

patients with metastatic carcinoid tumours [66]. It is still the most widely used somatostatin analogue for treatment of acromegaly, neuroendocrine tumours and gastrointestinal disorders in adult and in paediatric patients. Its primary advantages over somatostatin are a longer half-life (1.7–1.9 h vs. 2–3 mins) in the circulation, a higher potency, and good bioavailability. In humans, OCT is well tolerated with only minor possible side effects such as nausea and diarrhoea. In our rat and mice models, we did not observe any gross changes in physiological or behavioural parameters after acute OCT i.p. injection until animal perfusion, highlighting the interest of the use of OCT in our approach.

Assessment of OCT passage

Our results obtained by MRgFUS-BBB opening indicated a paracellular route of OCT passage into the brain. Indeed, this method utilizes the mechanical effect of microbubble oscillations which induced a transient disruption or loosening of the tight junctions in the brain endothelial cells thus facilitating paracellular permeability [41]. In addition, our *in vitro* model of human BBB also demonstrated the crossing of OCT through the endothelial monolayer by paracellular transport, in accordance with previous studies [57–59]. The juvenile cerebral ischaemia model, however, argues in favour of OCT being able to enter the brain through transcellular vesicular passage. Previous studies have demonstrated that transcytosis is increased in endothelial cells after stroke while the tight junctions remain generally intact during the first 24 h poststroke [67,68].

Regions of interest and limitations

Strong SST2 labelling is detected in the deep layers of the cerebral cortex, CA1 field and dentate gyrus of the hippocampus, lateral septum, medial septum/diagonal band of Broca, medial habenula, bed nucleus of the stria terminalis, endopiriform nucleus, claustrum, amygdaloid complex, arcuate nucleus, locus coeruleus and nucleus tractus solitarius [19,20,69]. Even in regions where the density of neurons expressing the SST2 receptor is lower (such as medial preoptic area or periventricular nucleus of the hypothalamus), following agonist-induced internalization in individual neurons (cell bodies and proximal dendrites) is always highly immunoreactive and easily detectable by classical immunohistochemical

procedures [22]. This phenomenon is explained by the fact that internalization induces intracellular concentration of receptors which increases the immunohistochemical signal detection. Although the SST2 is distributed in key brain structures for BBB research (such as the cerebral cortex, amygdala, striatum or hypothalamus: for a description see [19,20]), one limitation of our method is that this GPCR receptor is absent in some brain regions (such as cortical layer 1, dorsal thalamus or white matter). This method might, however, be suitable for other GPCRs that undergo ligand-induced internalization and are expressed in a particular region of interest. In such cases, receptor agonist should be chosen on the basis of their binding properties, aqueous solubility and molecular weight.

In conclusion, we have introduced a novel approach to study BBB integrity in embryo, juvenile and adult preclinical rodent models. Because of the high sensitivity and simplicity of our method, we anticipate that it could provide new opportunities for both pharmaceutical and academic laboratories to study BBB leakage in different pathological conditions, and to test the efficacy of various therapeutic strategies to protect or to open the BBB, especially during development.

Acknowledgements

This work was supported by Inserm, Paris Diderot University, La Fondation pour la Recherche sur le Cerveau, the PremUP Foundation, the Seventh Framework Program of the European Union Grant Agreement HEALTH-F2–2009-241778/Neurobid, the Bettencourt Schueller Foundation and the ‘Agence Nationale de la Recherche’ under the program ‘Future Investments’ with the reference ANR-10-EQPX-15. We thank Joanna Driesbeke and Nadège Sarrazin from the PHENOPARC Platform for their help with animal injections. The authors thank Dr Johan Pallud (Professor of neurosurgery at Paris Descartes University, Neurosurgeon at Sainte-Anne Hospital center, Paris, France) for providing fresh human brain sample from a patient suffering from oligodendroglioma.

Author contributions

Z.C. and T.V. designed, performed and interpreted experiments, prepared the figures, and contributed to the writing of the paper. C.C.-M., I.M., B.C., P.-L.L.,

I.P. designed, performed and interpreted experiments of the cerebral ischaemia model, C.C-M. also contributed to the writing of the paper. C.C., M.D.S., S.L., C.D., and J-F.A. designed, performed and interpreted experiments of the focused ultrasound-mediated BBB opening and contributed to the writing of the paper. A.J. designed, performed and interpreted experiments of the traumatic brain injury. N.P. F.G. designed, performed and interpreted experiments of the *in vitro* BBB model. L.T., S.A., M.T., J-F.G-E., H.A-B., J-F.A., P.G. were involved in the study design and interpretation of results. P.D. conceived and supervised the project, prepared the figures and wrote the paper.

Conflict of interest

The authors declare that they have no competing interests.

Ethics approval

The study was approved with permission from Inserm guidelines and the ethics committees on animal experiments of Paris Diderot University.

Consent for publication

All authors have read and approved the manuscript and agreed to publish in this journal.

Peer Review

The peer review history for this article is available at <https://publons.com/publon/10.1111/nan.12665>.

Data Availability Statement

The data that support the findings of this study are available from the corresponding author upon reasonable request.

References

- 1 Erickson MA, Banks WA. Neuroimmune axes of the blood-brain barriers and blood-brain interfaces: bases for physiological regulation, disease states, and pharmacological interventions. *Pharmacol Rev* 2018; **70**: 278–314
- 2 Obermeier B, Daneman R, Ransohoff RM. Development, maintenance and disruption of the blood-brain barrier. *Nat Med* 2013; **19**: 1584–96
- 3 Sweeney MD, Sagare AP, Zlokovic BV. Blood-brain barrier breakdown in Alzheimer disease and other neurodegenerative disorders. *Nat Rev Neurol* 2018; **14**: 133–50
- 4 Najjar S, Pahlajani S, De Sanctis V, Stern JNH, Najjar A, Chong D. Neurovascular unit dysfunction and blood-brain barrier hyperpermeability contribute to schizophrenia neurobiology: a theoretical integration of clinical and experimental evidence. *Front Psychiatry* 2017; **8**: 83
- 5 Najjar S, Pearlman DM, Devinsky O, Najjar A, Zagzag D. Neurovascular unit dysfunction with blood-brain barrier hyperpermeability contributes to major depressive disorder: a review of clinical and experimental evidence. *J Neuroinflammation* 2013; **10**: 142
- 6 Menard C, Pfau ML, Hodes GE, Kana V, Wang VX, Bouchard S, et al. Social stress induces neurovascular pathology promoting depression. *Nat Neurosci* 2017; **20**: 1752–60
- 7 Theoharides TC, Tsilioni I, Patel AB, Doyle R. Atopic diseases and inflammation of the brain in the pathogenesis of autism spectrum disorders. *Transl Psychiatry* 2016; **6**: e844
- 8 Moretti R, Pansiot J, Bettati D, Strazielle N, Ghersi-Egea JF, Damante G, et al. Blood-brain barrier dysfunction in disorders of the developing brain. *Front Neurosci* 2015; **9**: 40
- 9 Rudolph MD, Graham AM, Feczko E, Miranda-Dominguez O, Rasmussen JM, Nardos R, et al. Maternal IL-6 during pregnancy can be estimated from newborn brain connectivity and predicts future working memory in offspring. *Nat Neurosci* 2018; **21**: 765–772.
- 10 Wunder A, Schoknecht K, Stanimirovic DB, Prager O, Chassidim Y. Imaging blood-brain barrier dysfunction in animal disease models. *Epilepsia* 2012; **53**(Suppl 6): 14–21
- 11 Saunders NR, Dziegielewska KM, Mollgard K, Habgood MD. Markers for blood-brain barrier integrity: how appropriate is Evans blue in the twenty-first century and what are the alternatives? *Front Neurosci* 2015; **9**: 385
- 12 Hoffmann A, Bredno J, Wendland M, Derugin N, Ohara P, Wintermark M. High and low molecular weight fluorescein isothiocyanate (FITC)-dextran to assess blood-brain barrier disruption: technical considerations. *Transl Stroke Res* 2011; **2**: 106–11
- 13 Sohet F, Lin C, Munji RN, Lee SY, Ruderisch N, Soung A, et al. LSR/angulin-1 is a tricellular tight junction protein involved in blood-brain barrier formation. *J Cell Biol* 2015; **208**: 703–11
- 14 Ben-Zvi A, Lacoste B, Kur E, Andreone BJ, Mayshar Y, Yan H, et al. Mfsd2a is critical for the formation and function of the blood-brain barrier. *Nature* 2014; **509**: 507–11

- 15 Fernandez-Lopez D, Faustino J, Daneman R, Zhou L, Lee SY, Derugin N, et al. Blood-brain barrier permeability is increased after acute adult stroke but not neonatal stroke in the rat. *J Neurosci* 2012; **32**: 9588–600
- 16 Csaba Z, Lelouvier B, Viollet C, El Ghouzzi V, Toyama K, Videau C, et al. Activated somatostatin type 2 receptors traffic in vivo in central neurons from dendrites to the trans Golgi before recycling. *Traffic* 2007; **8**: 820–34
- 17 De Bundel D, Fafouri A, Csaba Z, Loyens E, Lebon S, El Ghouzzi V, et al. Trans-Modulation of the Somatostatin Type 2A Receptor Trafficking by Insulin-Regulated Aminopeptidase Decreases Limbic Seizures. *J Neurosci* 2015; **35**: 11960–75
- 18 Lelouvier B, Tamagno G, Kaindl AM, Roland A, Lelievre V, Le Verche V, et al. Dynamics of somatostatin type 2A receptor cargoes in living hippocampal neurons. *J Neurosci* 2008; **28**: 4336–49
- 19 Schindler M, Sellers LA, Humphrey PP, Emson PC. Immunohistochemical localization of the somatostatin SST2(A) receptor in the rat brain and spinal cord. *Neuroscience* 1997; **76**: 225–40
- 20 Dournaud P, Gu YZ, Schonbrunn A, Mazella J, Tanenbaum GS, Beaudet A. Localization of the somatostatin receptor SST2A in rat brain using a specific anti-peptide antibody. *J Neurosci* 1996; **16**: 4468–78
- 21 Le Verche V, Kaindl AM, Verney C, Csaba Z, Peineau S, Olivier P, et al. The somatostatin 2A receptor is enriched in migrating neurons during rat and human brain development and stimulates migration and axonal outgrowth. *PLoS One* 2009; **4**: e5509
- 22 Csaba Z, Simon A, Helboe L, Epelbaum J, Dournaud P. Targeting sst2A receptor-expressing cells in the rat hypothalamus through in vivo agonist stimulation: neuroanatomical evidence for a major role of this subtype in mediating somatostatin functions. *Endocrinology* 2003; **144**: 1564–73
- 23 Csaba Z, Simon A, Helboe L, Epelbaum J, Dournaud P. Neurochemical characterization of receptor-expressing cell populations by in vivo agonist-induced internalization: insights from the somatostatin sst2A receptor. *J Comp Neurol* 2002; **454**: 192–9
- 24 Pardridge WM. Drug transport across the blood-brain barrier. *J Cereb Blood Flow Metab* 2012; **32**: 1959–72
- 25 Marbach P, Briner U, Lemaire M, Schweitzer A, Terasaki T. From somatostatin to sandostatin: pharmacodynamics and pharmacokinetics. *Metabolism* 1992; **41**: 7–10
- 26 Tsai PS, Kaufhold JP, Blinder P, Friedman B, Drew PJ, Karten HJ, et al. Correlations of neuronal and microvascular densities in murine cortex revealed by direct counting and colocalization of nuclei and vessels. *J Neurosci* 2009; **29**: 14553–70
- 27 Fischer T, Doll C, Jacobs S, Kolodziej A, Stumm R, Schulz S. Reassessment of sst2 somatostatin receptor expression in human normal and neoplastic tissues using the novel rabbit monoclonal antibody UMB-1. *J Clin Endocrinol Metab* 2008; **93**: 4519–24
- 28 Magnin R, Rabusseau F, Salabartan F, Meriaux S, Aubry JF, Le Bihan D, et al. Magnetic resonance-guided motorized transcranial ultrasound system for blood-brain barrier permeabilization along arbitrary trajectories in rodents. *J Ther Ultrasound* 2015; **3**: 22
- 29 Leger PL, Pansiot J, Besson V, Palmier B, Renolleau S, Baud O, et al. Cyclooxygenase-2-Derived Prostaglandins Mediate Cerebral Microcirculation in a Juvenile Ischemic Rat Model. *Stroke* 2016; **47**: 3048–52
- 30 Chhor V, Moretti R, Le Charpentier T, Sigaut S, Lebon S, Schwendimann L, et al. Role of microglia in a mouse model of paediatric traumatic brain injury. *Brain Behav Immun* 2017; **63**: 197–209
- 31 Luo H, Gauthier M, Tan X, Landry C, Poupon J, Dehouck MP, et al. Sodium transporters are involved in lithium influx in brain endothelial cells. *Mol Pharm* 2018; **15**: 2528–38
- 32 Merzin M. Applying stereological method in radiology. Volume measurement. Bachelor's thesis. Bachelor's Thesis University of Tartu Estonia 2008
- 33 Schindelin J, Arganda-Carreras I, Frise E, Kaynig V, Longair M, Pietzsch T, et al. Fiji: an open-source platform for biological-image analysis. *Nat Methods* 2012; **9**: 676–82
- 34 Kaur C, Ling EA. The circumventricular organs. *Histol Histopathol* 2017; **32**: 879–92
- 35 Ciofi P. The arcuate nucleus as a circumventricular organ in the mouse. *Neurosci Lett* 2011; **487**: 187–90
- 36 Faouzi M, Leshan R, Bjornholm M, Hennessey T, Jones J, Munzberg H. Differential accessibility of circulating leptin to individual hypothalamic sites. *Endocrinology* 2007; **148**: 5414–23
- 37 Langlet F, Levin BE, Luquet S, Mazzone M, Messina A, Dunn-Meynell AA, et al. Tanycytic VEGF-A boosts blood-hypothalamus barrier plasticity and access of metabolic signals to the arcuate nucleus in response to fasting. *Cell Metab* 2013; **17**: 607–17
- 38 Kim KS, Seeley RJ, Sandoval DA. Signalling from the periphery to the brain that regulates energy homeostasis. *Nat Rev Neurosci* 2018; **19**: 185–96
- 39 Duerrschmid C, He Y, Wang C, Li C, Bournat JC, Romere C, et al. Asprosin is a centrally acting orexigenic hormone. *Nat Med* 2017; **23**: 1444–53
- 40 Reyes TM, Sawchenko PE. Involvement of the arcuate nucleus of the hypothalamus in interleukin-1-induced anorexia. *J Neurosci* 2002; **22**: 5091–9
- 41 Leinenga G, Langton C, Nisbet R, Gotz J. Ultrasound treatment of neurological diseases—current and emerging applications. *Nat Rev Neurol* 2016; **12**: 161–74
- 42 Meng Y, Suppiah S, Mithani K, Solomon B, Schwartz ML, Lipsman N. Current and emerging brain applications of MR-guided focused ultrasound. *J Ther Ultrasound* 2017; **5**: 26

- 43 Gunther T, Tulipano G, Dournaud P, Bousquet C, Csaba Z, Kreienkamp HJ, et al. International union of basic and clinical pharmacology. CV. Somatostatin Receptors: Structure, Function, Ligands, and New Nomenclature. *Pharmacol Rev* 2018; **70**: 763–835.
- 44 Tsze DS, Valente JH. Pediatric stroke: a review. *Emerg Med Int* 2011; **2011**: 734506
- 45 Jiang X, Andjelkovic AV, Zhu L, Yang T, Bennett MVL, Chen J, et al. Blood-brain barrier dysfunction and recovery after ischemic stroke. *Prog Neurobiol* 2017
- 46 Ma Q, Dasgupta C, Li Y, Huang L, Zhang L. MicroRNA-210 suppresses junction proteins and disrupts blood-brain barrier integrity in neonatal rat hypoxic-ischemic brain injury. *Int J Mol Sci* 2017; **18**
- 47 Hsu YC, Chang YC, Lin YC, Sze CI, Huang CC, Ho CJ. Cerebral microvascular damage occurs early after hypoxia-ischemia via nNOS activation in the neonatal brain. *J Cereb Blood Flow Metab* 2014; **34**: 668–76
- 48 Ek CJ, D'Angelo B, Baburamani AA, Lehner C, Leverin AL, Smith PL, et al. Brain barrier properties and cerebral blood flow in neonatal mice exposed to cerebral hypoxia-ischemia. *J Cereb Blood Flow Metab* 2015; **35**: 818–27
- 49 Gelot A, Villapol S, Billette de Villemeur T, Renolleau S, Charriaut-Marlangue C. Astrocytic demise in the developing rat and human brain after hypoxic-ischemic damage. *Dev Neurosci* 2009; **31**: 459–70
- 50 Giza CC, Mink RB, Madikians A. Pediatric traumatic brain injury: not just little adults. *Curr Opin Crit Care* 2007; **13**: 143–52
- 51 Alluri H, Wiggins-Dohlvik K, Davis ML, Huang JH, Tharakan B. Blood-brain barrier dysfunction following traumatic brain injury. *Metab Brain Dis* 2015; **30**: 1093–104
- 52 Saunders NR, Liddelow SA, Dziegielewska KM. Barrier mechanisms in the developing brain. *Front Pharmacol* 2012; **3**: 46
- 53 Csaba Z, Bernard V, Helboe L, Bluet-Pajot MT, Bloch B, Epelbaum J, et al. In vivo internalization of the somatostatin sst2A receptor in rat brain: evidence for translocation of cell-surface receptors into the endosomal recycling pathway. *Mol Cell Neurosci* 2001; **17**: 646–61
- 54 Daneman R, Zhou L, Kebede AA, Barres BA. Pericytes are required for blood-brain barrier integrity during embryogenesis. *Nature* 2010; **468**: 562–6
- 55 Caron P, Gerbeau C, Pradayrol L. Maternal-fetal transfer of octreotide. *N Engl J Med* 1995; **333**: 601–2
- 56 Fassnacht M, Capeller B, Arlt W, Steck T, Allolio B. Octreotide LAR treatment throughout pregnancy in an acromegalic woman. *Clin Endocrinol (Oxf)* 2001; **55**: 411–5
- 57 Jaehde U, Masereeuw R, De Boer AG, Fricker G, Nagelkerke JF, Vonderscher J, et al. Quantification and visualization of the transport of octreotide, a somatostatin analogue, across monolayers of cerebrovascular endothelial cells. *Pharm Res* 1994; **11**: 442–8
- 58 Abbruscato TJ, Thomas SA, Hruby VJ, Davis TP. Blood-brain barrier permeability and bioavailability of a highly potent and mu-selective opioid receptor antagonist, CTAP: comparison with morphine. *J Pharmacol Exp Ther* 1997; **280**: 402–9
- 59 Banks WA, Schally AV, Barrera CM, Fasold MB, Durham DA, Csernus VJ, et al. Permeability of the murine blood-brain barrier to some octapeptide analogs of somatostatin. *Proc Natl Acad Sci USA* 1990; **87**: 6762–6
- 60 Rapoport SI. Osmotic opening of the blood-brain barrier: principles, mechanism, and therapeutic applications. *Cell Mol Neurobiol* 2000; **20**: 217–30
- 61 Saunders NR, Dreifuss JJ, Dziegielewska KM, Johansson PA, Habgood MD, Mollgard K, et al. The rights and wrongs of blood-brain barrier permeability studies: a walk through 100 years of history. *Front Neurosci* 2014; **8**: 404
- 62 Yang S, Gu C, Mandeville ET, Dong Y, Esposito E, Zhang Y, et al. Anesthesia and Surgery Impair Blood-Brain Barrier and Cognitive Function in Mice. *Front Immunol* 2017; **8**: 902
- 63 Helboe L, Hay-Schmidt A, Stidsen CE, Moller M. Immunohistochemical localization of the somatostatin receptor subtype 2 (sst2) in the central nervous system of the golden hamster (*Mesocricetus auratus*). *J Comp Neurol* 1999; **405**: 247–61
- 64 Thoss VS, Piwko C, Hoyer D. Somatostatin receptors in the rhesus monkey brain: localization and pharmacological characterization. *Naunyn Schmiedeberg's Arch Pharmacol* 1996; **353**: 648–60
- 65 Csaba Z, Pirker S, Lelouvier B, Simon A, Videau C, Epelbaum J, et al. Somatostatin receptor type 2 undergoes plastic changes in the human epileptic dentate gyrus. *J Neuropathol Exp Neurol* 2005; **64**: 956–69
- 66 Weckbecker G, Lewis I, Albert R, Schmid HA, Hoyer D, Bruns C. Opportunities in somatostatin research: biological, chemical and therapeutic aspects. *Nat Rev Drug Discov* 2003; **2**: 999–1017
- 67 Knowland D, Arac A, Sekiguchi KJ, Hsu M, Lutz SE, Perrino J, et al. Stepwise Recruitment of Transcellular and Paracellular Pathways Underlies Blood-Brain Barrier Breakdown in Stroke. *Neuron* 2014; **82**: 603–17
- 68 Nahirney PC, Reeson P, Brown CE. Ultrastructural analysis of blood-brain barrier breakdown in the peri-infarct zone in young adult and aged mice. *J Cereb Blood Flow Metab* 2016; **36**: 413–25
- 69 Helboe L, Moller M, Norregaard L, Schiodt M, Stidsen CE. Development of selective antibodies against the human somatostatin receptor subtypes sst1-sst5. *Brain Res Mol Brain Res* 1997; **49**: 82–8

Supporting information

Additional Supporting Information may be found in the online version of this article at the publisher's web-site:

Data S1. SI Materials and Methods

Figure S1. Schematic representation of detection of increased blood-brain barrier (BBB) permeability using ligand-induced somatostatin receptor 2 (SST2) internalization.

Figure S2. Quantification of somatostatin receptor 2 (SST2) agonist extravasation after focused ultrasound-mediated (MRgFUS) disruption of the blood-brain barrier (BBB) in the cerebral cortex.

Figure S3. Characterization of cells with internalized somatostatin receptor 2 (SST2) following SST2 agonist extravasation in the rodent brain.

Figure S4. Characterization of somatostatin receptor 2 (SST2) localization in relation to blood vessels in the rodent brain.

Figure S5. Confocal microscopic analysis of somatostatin receptor 2 (SST2) immunoreactivity in the

periphery of E15.5 embryos following SST2 agonist injection of the dams.

Video S1. Low magnification 3D reconstruction of somatostatin receptor 2 (SST2) immunoreactivity in the mouse cerebral cortex following focused ultrasound-mediated (MRgFUS) opening of the blood-brain barrier (BBB).

Video S2. High magnification 3D reconstruction of somatostatin receptor 2 (SST2) immunoreactivity in the mouse cerebral cortex following focused ultrasound-mediated (MRgFUS) opening of the blood-brain barrier (BBB).

Received 28 January 2020

Accepted after revision 22 August 2020

Published online Article Accepted on 8 September 2020